Available online at www.sciencedirect.com
ScienceDirect
Trans. Nonferrous Met. Soc. China 31(2021) 2677−2686
Transactions of Nonferrous Metals Society of China
www.tnmsc.cn

Vacuum diffusion bonding of Ti_2AlNb alloy and TC4 alloy

Guang-jie FENG[1], Yan WEI[1], Bing-xu HU[1], Yi-feng WANG[1], De-an DENG[1], Xiu-xia YANG[2]

1. College of Materials Science and Engineering, Chongqing University, Chongqing 400044, China;
2. College of Land Resources and Environment, Jiangxi Agricultural University, Nanchang 330045, China

Received 30 October 2020; accepted 28 April 2021

Abstract: The Ti_2AlNb alloy was joined with TC4 alloy by vacuum diffusion bonding. The relationship between bonding parameters, and joint microstructure and shear strength was investigated. The results indicated that the diffusion of Al, Ti, Nb and V elements across bonding interface led to the formation of three reaction layers: *B*2/*β* layer and α_2 layer on the TC4 side, and α_2+*B*2/*β* layer on the Ti_2AlNb side. The bonding temperature determined the atomic activity, thus controlling the growth of reaction layers and influencing the shear strength of the joint. When the Ti_2AlNb alloy and TC4 alloy were bonded at 950 °C for 30 min under 10 MPa, the shear strength of the joint reached the maximum of 467 MPa. The analysis on the fracture morphology showed that the fracture occurred within the *B*2/*β* layer and the fracture model was ductile rupture. Meanwhile, the formation mechanism of the Ti_2AlNb/TC4 joint was discussed in depth.

Key words: Ti_2AlNb alloy; TC4 alloy; diffusion bonding; interfacial reaction; shear strength; formation mechanism

1 Introduction

Ti_2AlNb alloy possesses high specific strength and oxidation resistance, and outstanding creep resistance. It has been a promising structural material in automotive and aerospace fields [1−6]. In practical application, Ti_2AlNb alloy is inevitably required to join with other materials. TC4 alloy has been widely applied in aerospace fields beneficial from its low density, good workability, excellent corrosion resistance and outstanding fracture toughness [7,8]. The reliable joining of Ti_2AlNb alloy and TC4 alloy can produce composite structures with combined advantages, which is crucial for their engineering applications. It is foreseeable that the successful joining of Ti_2AlNb alloy and TC4 alloy is also a feasible way to further broaden their applications.

Various joining methods have been employed to join Ti_2AlNb alloy with itself or other materials [9−11]. LEI et al [12] investigated the laser welding of Ti_2AlNb alloy and compared the microstructure and tensile properties of the joint with those of the joint obtained by laser-additive welding. LI et al [13] investigated the electron beam welding of Ti_2AlNb alloy. Their results indicated that when the Ti_2AlNb alloy was welded by fusion welding methods, it was difficult to control the joint microstructure and avoid the defects (e.g. cracks and pores) without post-weld heat treatment. The transient liquid phase (TLP) bonding and brazing methods have also been applied to welding Ti_2AlNb alloy. CAI et al [14] and ZOU et al [15] investigated the TLP bonding of Ti_2AlNb alloy using the Ti−Ni interlayer and Ti−Ni−Cu interlayer, respectively. WANG et al [16,17] brazed the Ti_2AlNb alloy using the Ti−Ni−Nb filler metals. Their study suggested that the Nb content determined the dissolving of

Corresponding author: Guang-jie FENG, Tel: +86-18945690626, E-mail: fenggj@cqu.edu.cn;
DOI: 10.1016/S1003-6326(21)65684-4

Ti_2AlNb substrate, thus influencing the joint microstructure and mechanical properties. REN et al [18] brazed Ti_2AlNb alloy using the TiZrNiCu(Co) filler metals. HAO et al [19] developed AgCu-based filler metals to braze the Ti_2AlNb alloy to C/C composites. The above studies indicated that joints could be achieved through the optimization of process parameters. But since the filler metals and interlayers were usually Ti-based alloys, brittle IMCs (intermetallic compounds) were inevitably formed in the joints, which might turn into the possible microcrack source during the service process. Moreover, a high joining temperature was generally needed owing to the high melting point of Ti-based alloy, which led to the degradation of material's properties.

As one kind of solid-state bonding techniques, diffusion bonding has some inherent advantages compared with other joining methods. Thus, diffusion bonding can successfully be used to join titanium alloys, in general including the Ti_2AlNb alloy [20−31]. LI et al [26] and ALEGRIA et al [27] pointed out that diffusion bonding technique was suitable for joining materials with minimum metallurgical deterioration and yielding sound joints without post-weld heat treatment. Therefore, diffusion bonding has been regarded as an appropriate method to join Ti_2AlNb alloy. ZHU et al [28] investigated the diffusion bonding of Ti_2AlNb alloy and high Nb containing TiAl alloy. Results indicated that the bonding parameters influenced the thickness and composition of reaction layers at bonding interface, thus determining the mechanical performance of the joint. WANG et al [29] studied the vacuum diffusion bonding of Ti_2AlNb alloy using a Ti interlayer. It is suggested that the bonding parameter controlled the diffusion of Nb element towards the Ti interlayer, and influenced the characteristics of diffusion zones. REN et al [30] realized the joining of Ti_2AlNb alloy and Ni-based superalloy by nano-diffusion bonding. They proposed that the Cu/Ti nano-laminated foils had a higher activity than conventional interlayers and nano-diffusion bonding was suitable for joining the dissimilar materials. WANG et al [31] achieved the hydrogenated niobium foil by cathodic charging and used it as the interlayer in the diffusion bonding of Ti_2AlNb alloy and TiAl alloy. Although great efforts have been made, most of them were mainly focused on the optimization of bonding parameters. The diffusion bonding mechanism of Ti_2AlNb alloy and TC4 alloy has rarely been discussed.

As a fundamental research, the feasibility of diffusion bonding of Ti_2AlNb alloy to TC4 alloy was studied in the present work. Through analyzing the joint microstructure and shear strength with different bonding parameters, the relationship between bonding parameters, and microstructure and shear strength of the joint was systematically investigated. Meanwhile, the formation mechanism of Ti_2AlNb/TC4 diffusion bonded joint was discussed in depth, thus providing a theoretical basis and guidance in the practical applications of Ti_2AlNb alloy and TC4 alloy.

2 Experimental

Figure 1 shows the microstructures of Ti_2AlNb alloy and TC4 alloy. The Ti_2AlNb alloy was in the as-cast status and had a chemical composition of Ti−22Al−23Nb−2V (at.%). It consisted of three phases: $B2$, O and α_2. TC4 alloy had a chemical composition of Ti−6Al−4V (at.%) and featured a dual-phase structure of grey α matrix phase and white β phase.

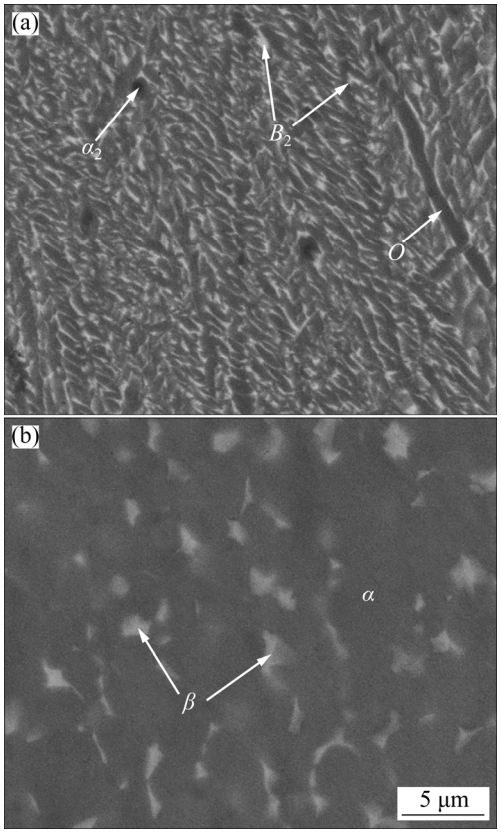

Fig. 1 Microstructures of Ti_2AlNb (a) and TC4 (b) alloys

Before diffusion bonding, the Ti_2AlNb and TC4 substrates were cut into small pieces by the wire-cut electrical discharge machining. The sizes of Ti_2AlNb and TC4 substrates were 6 mm × 5 mm × 3 mm and 10 mm × 8 mm × 1.9 mm, respectively. Then, the joining surfaces were polished by SiC papers up to 1200#. Finally, all the samples were placed in acetone and cleaned for 10 min under ultrasound. The bonding couples were fixed in a graphite jig and the bonding pressure was 10 MPa. The diffusion bonding experiment was performed in a vacuum furnace. The vacuum level was about 4×10^{-4} Pa. The heating rate was 30 °C/min. When the holding time was over, the bonding couple was first cooled down to 400 °C at a cool rate of 15 °C/min. Then, the heat power was turned off and the bonding couple was cooled down to room temperature in furnace.

After the diffusion bonding, the joint was cut into halves along the center line and was inlaid in base polymer. Then, the specimens were polished by SiC papers and diamond polishing agent. The cross-section and the fracture surface of joints were characterized using the scanning electron microscope (SEM) equipped with the energy-dispersive spectrometer (EDS), and X-ray diffractometer (XRD). The room-temperature shear strength of the joint was tested using the universal test machine. The shear rate was 0.5 mm/min. The schematic diagram is shown in Fig. 2.

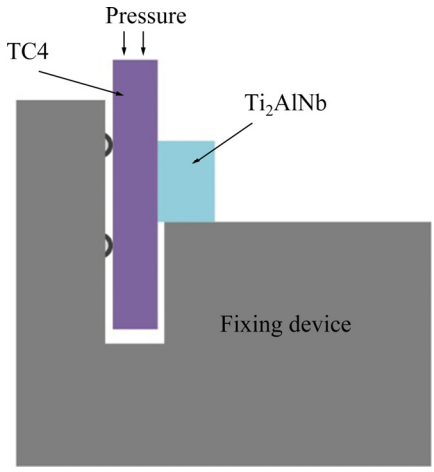

Fig. 2 Schematic diagram of joint shear test

3 Results and discussion

3.1 Typical microstructure of Ti_2AlNb/TC4 joint

Figure 3 shows the typical microstructure of the Ti_2AlNb/TC4 joint bonded at 950 °C for 30 min under a pressure of 10 MPa. The SEM back-scattered electron (BSE) image revealed that the Ti_2AlNb alloy was bonded well to TC4 alloy. Three distinctive zones were formed at the bonding interface, as marked in Fig. 3. The diffusion Zone I was composed primarily of a grey big blocky phase (marked as A). The diffusion Zone II was a continuous dark grey layer (marked as B). The diffusion Zone III contained a grey matrix phase (marked as C) and a dark grey granular phase (marked as D). EDS analysis was conducted on each phase. According to EDS results in Table 1 and Ti−Al−Nb ternary phase diagram, the grey big blocky phase (i.e. Phase A) in Zone I and the grey matrix phase (Phase C) in Zone III were supposed to be the *B2*/*β* phase. The dark grey layer (Phase B) in Zone II and the dark grey granular phase (Phase C) in Zone III were the α_2 phases. To further confirm the phases in the joint, XRD analysis was also carried out. The results in Fig. 4(a) showed the existence of α_2 and *B2*/*β* phases and proved above analysis.

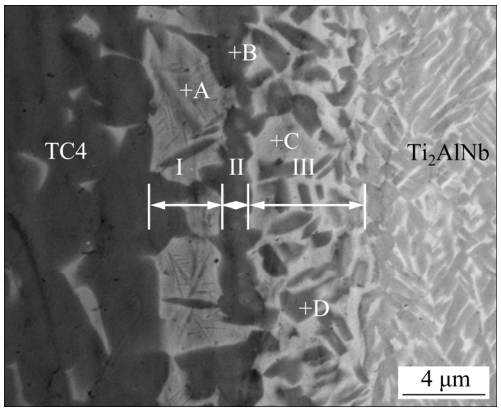

Fig. 3 Typical microstructure of Ti_2AlNb/TC4 joint (950 °C, 30 min and 10 MPa)

Table 1 EDS results of each phase in Fig. 3 (at.%)

Position	Ti	Al	Nb	V	Phase
A	74.61	12.65	8.46	4.29	*B2*/*β*
B	70.06	21.97	6.68	1.29	α_2
C	64.26	15.00	17.16	3.58	*B2*/*β*
D	63.89	22.19	11.42	2.51	α_2

Figure 4(b) represents the elemental line distributions across the joint. Compared with Ti_2AlNb alloy, TC4 alloy had a high content of Ti and V, and a low content of Nb and Al. Driven by

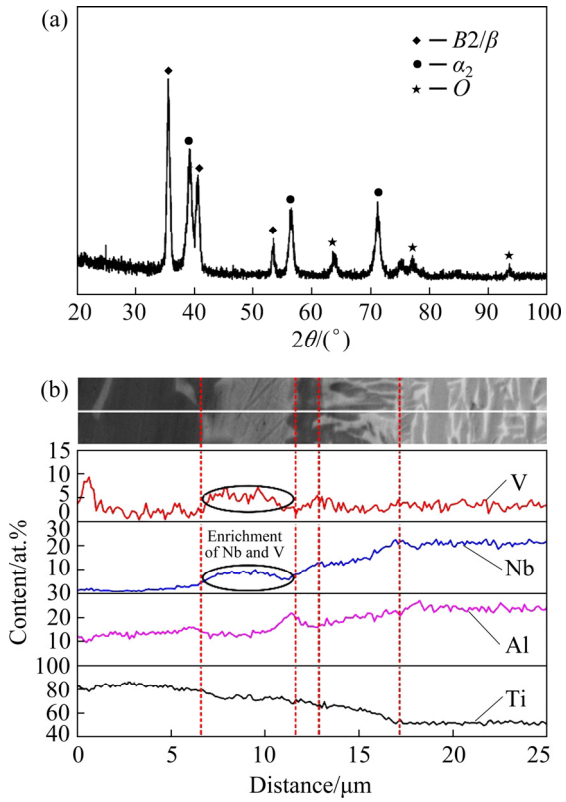

Fig. 4 XRD pattern (a) and elemental line distribution (b)

the chemical concentration gradient, V and Ti atoms migrated from the TC4 substrate to Ti_2AlNb substrate, while Nb and Al atoms diffused along the opposite direction. It should be noticed that the distributions of Nb, V and Al elements were obviously selective in the vicinity of bonding interface. In Zone I, Nb and V elements had an apparent enrichment while Al concentrate decreased. This phenomenon was mainly due to the different roles of Nb, V and Al elements in the phase transformation process. ZHAO et al [32] reported that Nb and V were the β-stabilising elements, and HUANG et al [33] reported that Al was the α-stabilising element. During the diffusion bonding, Nb and Al atoms diffused from Ti_2AlNb substrate to TC4 substrate. Nb atoms aggregated in the primary β phase in the TC4 substrate, promoting the formation of $B2/\beta$ phase in Zone I. Al atoms aggregated in the primary α phase, forming the dark grey α_2 layer. Meanwhile, Ti atoms diffused from TC4 substrate to Ti_2AlNb substrate. The increase of Ti concentrate in Ti_2AlNb alloy was beneficial to the formation of α_2 phase. A small portion of α_2 phase with a granular morphology precipitated from the primary microstructure during the diffusion bonding, forming the $B2/\beta+\alpha_2$ microstructure in Zone III. Thus, it could be inferred that Zones I and II were the diffusion zones formed from the TC4 alloy, and Zone III was the diffusion zone formed from the Ti_2AlNb alloy.

3.2 Influence of bonding parameters on joint microstructure

Figure 5 shows the joint microstructure at different bonding temperatures. With the increase of bonding temperature, the interfacial microstructure had a dramatic change. During the diffusion bonding process, the atomic diffusion velocity (D)

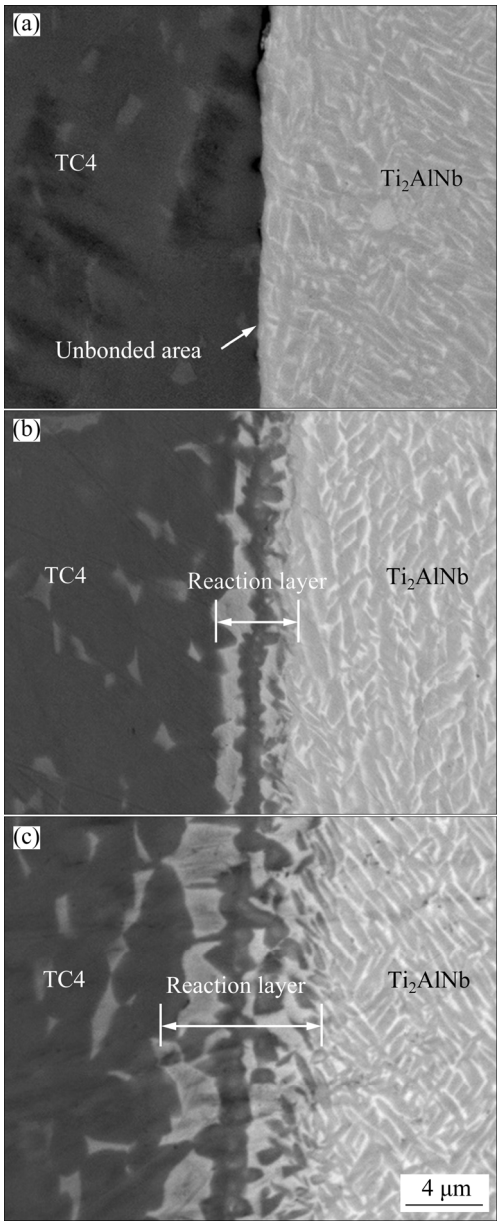

Fig. 5 Influence of bonding temperature on joint microstructure (10 min and 10 MPa): (a) 800 °C; (b) 900 °C; (c) 950 °C

followed the Arrhenius equation [34]:

$$D = D_0 \exp(\frac{-Q}{RT}) \quad (1)$$

where D_0, Q, R and T are the diffusion coefficient, activation energy, gas constant and temperature, respectively.

The atomic mobility was positively correlated with elevated temperature [35,36]. The inter-diffusion of Ti, Al, Nb and V elements determined the formation of reaction layers at the Ti_2AlNb/TC4 interface. When the bonding temperature was 800 °C, the low atomic mobility led to the insufficient elemental diffusion and the short diffusion distance in the bonding couple. No continuous reaction layer could be formed at the bonding interface. The unbonded area was observed clearly in Fig. 5(a). When the bonding temperature increased to 900 °C, the mutual diffusion of Ti, Al, Nb and V elements was enhanced at the bonding interface. The interfacial reactions were promoted partly. Therefore, continuous reaction layers were formed in the joint (see Fig. 5(b)). The total thickness of four reaction layers was ~4 μm. Further increase of bonding temperature to 950 °C greatly enhanced the atomic mobility. The interfacial reaction layers continued to grow, and the thickness of reaction layers increased from 4 to 8 μm.

Figure 6 shows the interfacial microstructure evolution with different holding time. Unlike the obvious increasing trend in Fig. 5, the thickness of interfacial reaction layers showed a very slow increase with the prolonging of holding time. When the holding time increased from 10 to 60 min, the total thickness of reaction layers only increased from 8 to 11 μm. Thus, the growth of reaction layers in Ti_2AlNb/TC4 joint was more sensitive to and likely to be influenced by the bonding temperature rather than the holding time. This phenomenon could be explained as follows. In diffusion bonding, the formation process of interfacial reaction layers consisted of two parts: atomic diffusion process and chemical reaction process. For the diffusion bonding of Ti_2AlNb alloy and TC4 alloy, the atomic diffusion time was far longer than the chemical reaction time, and the growth of reaction layers was mainly determined by the atomic diffusion. High bonding temperature provided the atoms more energy to overcome the energy barrier in the diffusion process and get a long diffusion distance. YAO et al [37] suggested that within a rational degree, a thicker reaction layer might lead to the higher mechanical properties. Therefore, a high bonding temperature was required to realize the reliable bonding of Ti_2AlNb alloy and TC4 alloy.

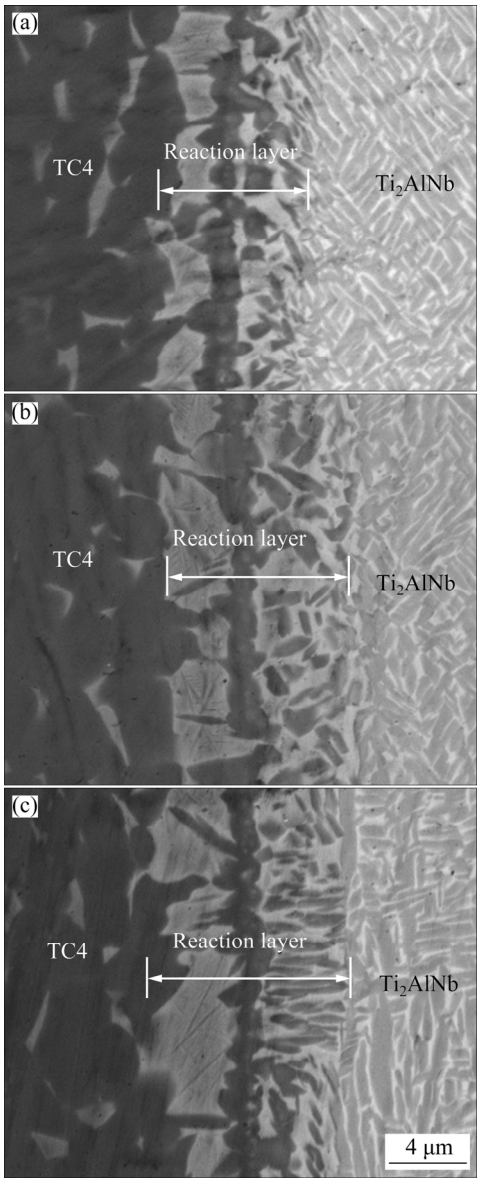

Fig. 6 Influence of bonding time on joint microstructure (950 °C and 10 MPa): (a) 10 min; (b) 30 min; (c) 60 min

3.3 Shear strength of Ti_2AlNb/TC4 joints

The room-temperature shear strength test was performed to evaluate the mechanical properties of the Ti_2AlNb/TC4 joints. Figure 7 shows the tested results of the joints bonded with different parameters. It could be seen from Fig. 7(a) that the bonding temperature had a dramatic influence on

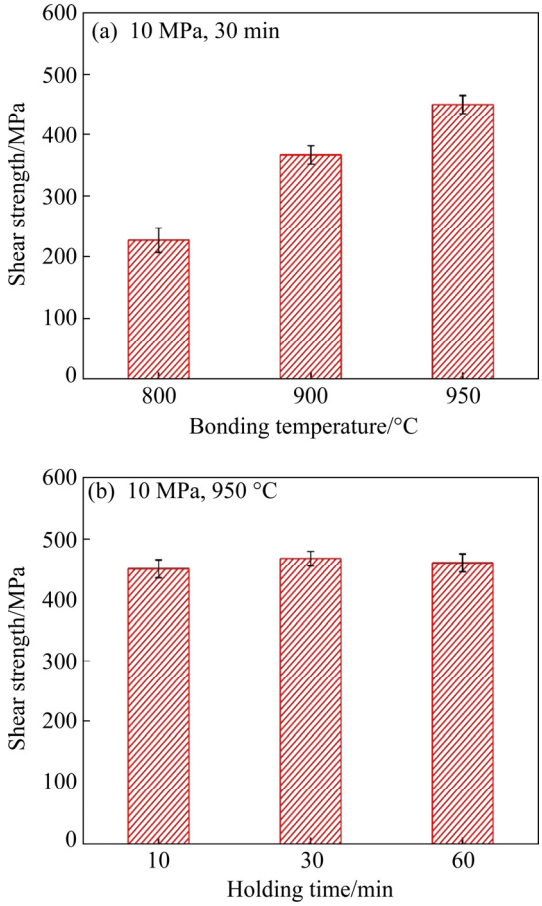

Fig. 7 Influence of bonding temperature (a) and holding time (b) on shear strength of Ti_2AlNb/TC4 joints

the shear strength of the joint. When the bonding temperature was 800 °C, the shear strength was 227 MPa. When the bonding temperature increased to 900 and 950 °C, the shear strength first reached 367 MPa and then the maximum value of 450 MPa. The variation of shear strength of the joint depended on the evolution of joint microstructure [38,39]. Figure 5 indicated that when the bonding temperature was 800 °C, the elemental interdiffusion was insufficient and no reaction layer was formed at the bonding interface. The unbonded area was clearly observed, leading to the low shear strength. Increasing the bonding temperature improved the atomic mobility. More Ti, Al and Nb atoms moved across the interface and entered the adjacent substrate. The thickness of reaction layers reached 4 μm when the bonding temperature increased to 900 °C, which effectively improved the bonding quality. As a result, the shear strength of the joint increased from 227 to 367 MPa. When the bonding temperature further increased to 950 °C, the reaction layers grew thicker. The total thickness of the reaction layers reached 8 μm. Beneficial from the thick reaction layers, the joint could bear higher load during the shear test. The shear strength of the joint reached the maximum of 450 MPa.

Figure 7(b) displays the shear strength of the joints bonded with different holding time. Unlike the results in Fig. 7(a), the holding time had a very slight influence on the shear strength of the joint. When the holding time increased from 10 to 60 min, the shear strength fluctuated between 450 and 467 MPa, maintaining at a high level. It was mainly because when the bonding temperature was 950 °C, the atomic activities of Ti, Al and Nb elements were already very high. Even the holding time was as short as 10 min, reaction layers with a total thickness of 8 μm still could be formed at the bonding interface. When the holding time reached 30 min, the reaction layers grew thicker. But the total thickness of reaction layers only increased by 2 μm and reached 10 μm. Within certain limits, thicker reaction layers were favorable to the mechanical performance of the joint [40]. Thus, the shear strength of the joint increased to 467 MPa. However, the reaction layers had brittle IMCs and large property difference (e.g. CTE) with the Ti_2AlNb and TC4 substrates. When the reaction layers were too thick, high residual stress was formed at the bonding interface and affected the joint strength. Therefore, when the holding time was 60 min, the total thickness of reaction layers increased to 12 μm. The shear strength of the joint slightly decreased to 460 MPa. It was noteworthy that when the bonding temperature was 950 °C, the shear strength of the joints was all higher than 450 MPa with different holding time, which was also higher than that of the Ti_2AlNb joints obtained by brazing (359 MPa) [17] and TLP bonding (428 MPa) [14]. Additionally, the high-strength diffusion bonding joint of Ti_2AlNb alloy and TC4 alloy could be achieved with a wide range of bonding parameters, which was crucial for the engineering application [29].

Figure 8 shows the fracture morphology of Ti_2AlNb/TC4 joint obtained at 950 °C for 30 min under a pressure of 10 MPa. It could be seen from Fig. 8(a) that the joint fracture surface had a flat morphology, which meant that the fracture might occur within the same reaction zone. To confirm the fracture mode, a typical position in Fig. 8(a) was enlarged to show more details. In the magnified

image (see Fig. 8(b)), dimple-like structures were observed, which meant that the dominant joint fracture mode was ductile rupture. Corresponding EDS analysis was also performed on the fracture surface. The results (76.74 at.% Ti, 13.12 at.% Al, 9.01 at.% Nb and 1.13 at.% V) demonstrated that the fracture was supposed to occur within Zone I (*B*2/*β*).

3.4 Formation mechanism of joint

The above analysis indicated that the elemental diffusion during the bonding process determined the interfacial microstructure of the joint. To illustrate the microstructure evolution of the joint, a physical model was established (see Fig. 9). The formation of the Ti_2AlNb/TC4 joint could be divided into the following four stages.

(1) Physical contact

Prior to the diffusion bonding, the bonding couple was fixed under a certain bonding pressure. Although the bonding surfaces were polished by the sand paper, they were still uneven on the meta-microscale and cannot get full contact with each other. Some voids were formed at the bonding interface, as shown in Fig. 9(a). With the elevation of temperature, the Ti_2AlNb alloy and TC4 alloy became soft gradually. Under the effect of bonding pressure, deformation and flow occurred in the substrates near the interface, which significantly increased the contact area. The voids at the interface disappeared gradually and the substrates got full contact with each other.

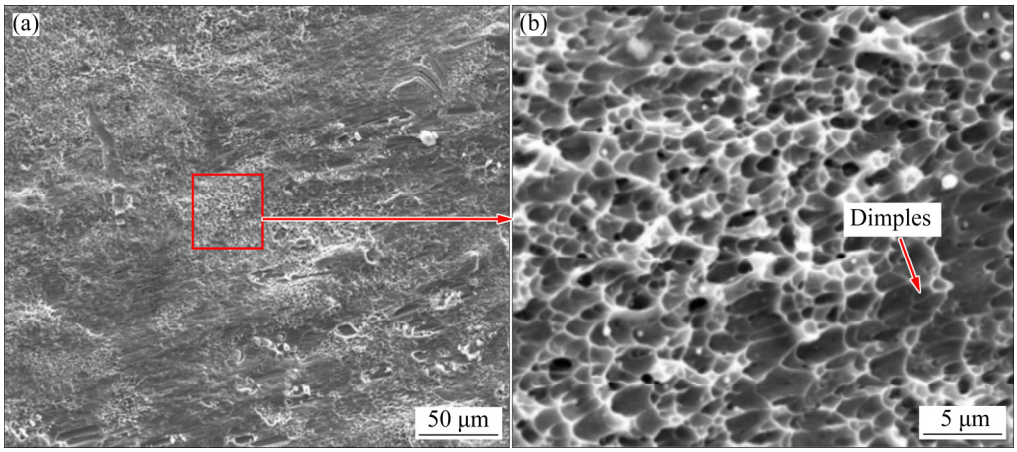

Fig. 8 Fracture surface morphologies of Ti_2AlNb/TC4 joint

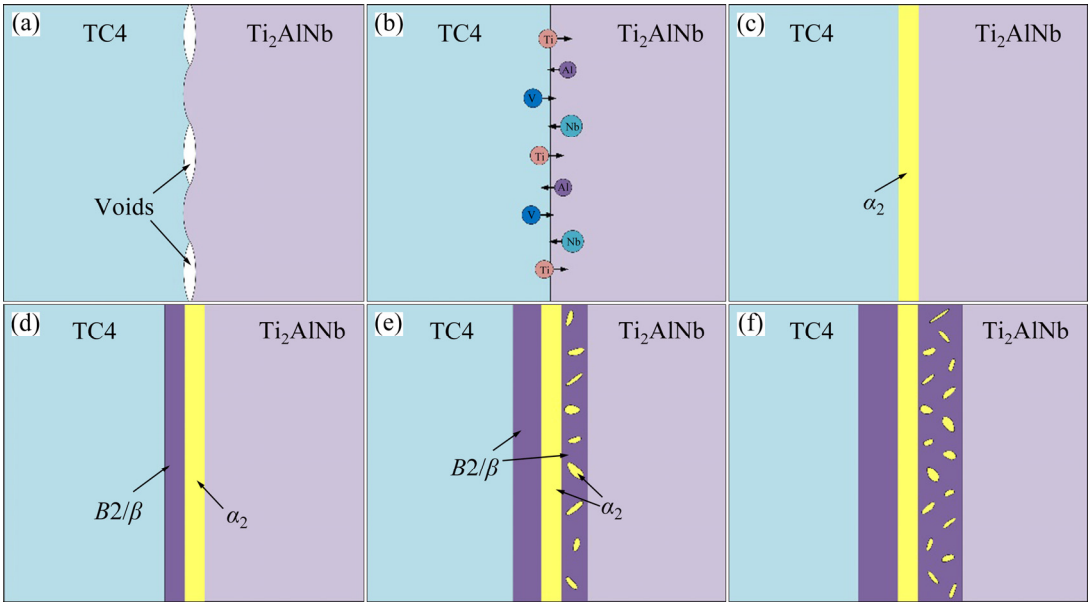

Fig. 9 Schematic diagrams of formation mechanism of Ti_2AlNb/TC4 diffusion bonded joint: (a) Physical contact; (b) Atomic diffusion; (c−e) Formation of reaction layers; (f) Growth of reaction layers

(2) Atomic diffusion

When the bonding temperature increased to the set value, the substrates got full contact with each other. The increased contact area was beneficial to the elemental diffusion. Due to different chemical compositions of the Ti_2AlNb alloy and TC4 alloy, there was a concentration gradient of Ti, Al, Nb and V elements at the bonding interface. Under the driving force of this concentration gradient, Ti and V elements from TC4 alloy moved across the interface and diffused into the Ti_2AlNb alloy. Meanwhile, the Ti_2AlNb alloy had high contents of Al and Nb elements. The Al and Nb elements spontaneously diffused into the TC4 alloy, as shown in Fig. 9(b).

(3) Formation of reaction layers

With the diffusion bonding progressed, a large number of atoms exchanged through the interface, forming a diffusion zone. Driven by the chemical concentration gradient, Al and Nb elements diffused into the TC4 alloy. In the narrow region near the interface, Al and Nb concentrations increased obviously. Figure 1 shows that the TC4 alloy had a dual-phase structure of α matrix and blocky β. High Al concentration promoted the $\alpha \rightarrow \alpha_2$ phase transformation in α matrix. A thin α_2 reaction layer was formed, as shown in Fig. 9(c). Since Nb and V were the β-stabilising elements, the increasing Nb concentration promoted the growth of blocky β phase in TC4 alloy. As the atomic diffusion went on, the blocky β phase grew up gradually and linked up, forming a reaction layer, as shown in Fig. 9(d). Meanwhile, the growth of β phase needed more Nb atoms, so the Nb atoms spontaneously migrated from α_2 layer and concentrated in the $B2/\beta$ layer, which could be seen from the elemental line distribution in Fig. 4(b). On the Ti_2AlNb side, the decrease of Nb and Al concentrations and the increase of Ti concentration transformed the triphase structure of α_2+O+B2 to the dual-phase structure of $B2+\alpha_2$ near the interface. As for the V element, it had a less effect on the phase transformation during the diffusion bonding because of its low content. Thus, it was not discussed in this section.

(4) Growth of reaction layers

After the main reaction layers were formed in the bonding couple, the interfacial structure became stable. In the holding period, the atomic diffusion kept going and the reaction layers grew thicker. A reliable metallurgical bonding was formed between Ti_2AlNb alloy and TC4 alloy. When the holding process was over, the bonding couple cooled down in the furnace. The atomic diffusion in the joint gradually stopped, forming the final joint, as shown in Fig. 9(f).

4 Conclusions

(1) The distributions of Nb, V and Al elements were selective at the bonding interface. The interfacial microstructure of the Ti_2AlNb/TC4 joint was characterized by three reaction layers: $B2/\beta$ layer (I) and α_2 layer (II) on the TC4 side, and α_2+B2/β layer (III) on the Ti_2AlNb side.

(2) The bonding parameters determined the atomic activity in the bonding couple, thus influencing the formation and growth of the interfacial reaction layers. The bonding temperature had a much more significant influence on the microstructure evolution of the joint than the bonding time.

(3) When the Ti_2AlNb alloy and TC4 alloy were bonded at 950 °C for 30 min under a pressure of 10 MPa, the elemental diffusion was sufficient and the shear strength of the joint had the maximum value of 467 MPa. The fracture occurred within the $B2/\beta$ layer and the fracture model was the ductile rupture.

(4) The formation of Ti_2AlNb/TC4 diffusion bonded joint consisted of four stages: physical contact, atomic diffusion, formation of reaction layers and growth of reaction layers.

Acknowledgments

This work was supported by the National Natural Science Foundation of China (No. 51905055), the Natural Science Foundation of Chongqing, China (No. cstc2020jcyj-msxmX0115) and the Fundamental Research Funds for the Central Universities, China (No. 2020CDJ-LHZZ-086).

References

[1] LI Yan-jun, WU Ai-ping, LI Quan, ZHAO Yue, ZHU Rui-can, WANG Guo-qing. Mechanism of reheat cracking in electron beam welded Ti2AlNb alloys [J]. Transactions of Nonferrous Metals Society of China, 2019, 29(9):

1873−1881.

[2] ESIN V A, MALLICK R, DADÉ M, DENAND B, DELFOSSE J, SALLOT P. Combined synchrotron X-ray diffraction, dilatometry and electrical resistivity in situ study of phase transformations in a Ti_2AlNb alloy [J]. Materials Characterization, 2020, 169: 110654.

[3] HE Yong-sheng, HU Rui, LUO Wen-zhong, HE Tao, LAI Yun-jin, DU Yu-jun, LIU Xiang-hong. Microstructural evolution and creep deformation behavior of novel Ti−22Al−25Nb−1Mo−1V−1Zr−0.2Si (at.%) orthorhombic alloy [J]. Transactions of Nonferrous Metals Society of China, 2019, 29(2): 313−321.

[4] ZHANG Ya-ran, LIU Yong-chang, YU Li-ming, LIANG Hong-yan, HUANG Yuan, MA Zong-qing. Microstructures and tensile properties of Ti_2AlNb and Mo-modified Ti_2AlNb alloys fabricated by hot isostatic pressing [J]. Materials Science and Engineering A, 2020, 776: 139043.

[5] DADÉ M, ESIN V A, NAZÉ L, SALLOT P. Short- and long-term oxidation behaviour of an advanced Ti_2AlNb alloy [J]. Corrosion Science, 2019, 148: 379−387.

[6] SUN Yu, ZHANG Heng, WAN Zhi-peng, REN Li-li, HU Lian-xi. Establishment of a novel constitutive model considering dynamic recrystallization behavior of Ti−22Al−25Nb alloy during hot deformation [J]. Transactions of Nonferrous Metals Society of China, 2019, 29(3): 546−557.

[7] CUI Shu-wan, SHI Yong-hua, ZHANG Cheng-shi. Microstructure and mechanical properties of TC4 titanium alloy K-TIG welded joints [J]. Transactions of Nonferrous Metals Society of China, 2021, 31(2): 416−425.

[8] XU Wei-feng, MA Jun, LUO Yu-xuan, FANG Yue-xiao. Microstructure and high-temperature mechanical properties of laser beam welded TC4/TA15 dissimilar titanium alloy joints [J]. Transactions of Nonferrous Metals Society of China, 2020, 30(1): 160−170.

[9] LI Ping, WANG Lu-sheng, YAN Si-liang, MENG Miao, XUE Ke-min. Temperature effect on the diffusion welding process and mechanism of *B*2−*O* interface in the Ti_2AlNb-based alloy: A molecular dynamics simulation [J]. Vacuum, 2019, 173: 109118.

[10] LI Yan-jun, WU Ai-ping, LI Quan, ZHAO Yue, ZHU Rui-can, WANG Guo-qing. Effects of welding parameters on weld shape and residual stresses in electron beam welded Ti_2AlNb alloy joints [J]. Transactions of Nonferrous Metals Society of China, 2019, 29(1): 67−76.

[11] CHEN X, XIE F Q, MA T J, LI W Y, WU X Q. Microstructural evolution and mechanical properties of linear friction welded Ti_2AlNb joint during solution and aging treatment [J]. Materials Science and Engineering A, 2016, 668: 125−136.

[12] LEI Zheng-long, ZHANG Ke-zhao, ZHOU Heng, NI Long-chang, CHEN Yan-bin. A comparative study of microstructure and tensile properties of Ti_2AlNb joints prepared by laser welding and laser-additive welding with the addition of filler powder [J]. Journal of Materials Processing Technology, 2018, 255: 477−487.

[13] LI Yan-jun, ZHAO Yue, LI Quan, WU Ai-ping, ZHU Rui-can, WANG Guo-qing. Effects of welding condition on weld shape and distortion in electron beam welded Ti_2AlNb alloy joints [J]. Materials & Design, 2017, 114: 226−233.

[14] CAI X Q, WANG Y, YANG Z W, WANG D P, LIU Y C. Transient liquid phase (TLP) bonding of Ti_2AlNb alloy using Ti/Ni interlayer: Microstructure characterization and mechanical properties [J]. Journal of Alloys and Compounds, 2016, 679: 9−17.

[15] ZOU Gui-sheng, XIE Er-hu, BAI Hai-lin, WU Ai-ping, WANG Qing, REN Jia-lie. A study on transient liquid phase diffusion bonding of Ti−22Al−25Nb alloy [J]. Materials Science and Engineering A, 2009, 499: 101−105.

[16] WANG Y, CAI X Q, YANG Z W, QIU Q W, WANG D P, LIU Y C. Microstructure evolution and mechanical properties of Ti−22Al−25Nb alloy joints brazed with Ti−Ni−Nb alloy [J]. Materials Chemistry and Physics, 2016, 182: 488−497.

[17] WANG Y, CAI X Q, YANG Z W, WANG D P, LIU X G, LIU Y C. Effects of Nb content in Ti−Ni−Nb brazing alloys on the microstructure and mechanical properties of Ti−22Al−25Nb alloy brazed joints [J]. Journal of Materials Science & Technology, 2017, 33: 682−689.

[18] REN H S, XIONG H P, CHEN B, PANG S J, CHEN B Q, YE L. Vacuum brazing of Ti_3Al-based alloy to TiAl using TiZrCuNi(Co) fillers [J]. Journal of Materials Processing Technology, 2015, 224: 26−32.

[19] HAO Zhi-tao, WANG Dong-po, YANG Zhen-wen, WANG Ying. Microstructure and mechanical properties of Ti2AlNb alloy and C/C composite joints brazed with Ag−Cu−Zn and Ag−Cu−Zn/Cu/Ag−Cu−Ti filler metals [J]. Archives of Civil and Mechanical Engineering, 2019, 19: 1083−1094.

[20] ÇAM G, CLEMENS H, GERLING R, KOÇAK M. Diffusion bonding of fine grained gamma-TiAl sheets [J]. Zeitschrift fuer Metallkunde, 1999, 90(4): 284−288.

[21] ÇAM G, BOHM K H, MÜLLAUER J, KOÇAK M. The fracture behavior of diffusion-bonded duplex gamma TiAl [J]. JOM: The Journal of the Minerals, Metals & Materials Society, 1996, 48(11): 66−68.

[22] ÇAM G, MÜLLAUER J, KOÇAK M. Diffusion bonding of two phase γ-TiAl alloys with duplex microstructure [J]. Science and Technology of Welding and Joining, 1997, 2(5): 213−219.

[23] ÇAM G, ÖZDEMIR U, VENTZKE V, KOÇAK M. Microstructural and mechanical characterization of diffusion bonded hybrid joints [J]. Journal of Materials Science, 2008, 43(10): 3491−3499.

[24] ÇAM G, IPEKOĞLU G, BOHM K H, KOÇAK M. Investigation into the microstructure and mechanical properties of diffusion bonded TiAl alloys [J]. Journal of Materials Science, 2006, 41(16): 5273−5282.

[25] KOÇAK M, PAKDIL M, ÇAM G. Fracture behaviour of diffusion bonded Ti-alloys with strength mismatch [J]. Science and Technology of Welding and Joining, 2002, 7(4): 187−196.

[26] LI Peng, WANG Shuai, XIA Yue-qing, HAO Xiao-hu, DONG Hong-gang. Diffusion bonding of AlCoCrFeNi2.1 eutectic high entropy alloy to TiAl alloy [J]. Journal of Materials Science & Technology, 2020, 45: 59−69.

[27] ALEGRIA J, MIRANDA R M, MARIA G D S J, FERNANDES A A. Modelling of voids closure in the

diffusion bonding process [J]. Materials Science Forum, 2008, 587−588: 731−735.
[28] ZHU Lei, LI Jin-shan, TANG Bin, LIU Yan, ZHANG Meng-qi, LI Lei, KOU Hong-chao. Microstructure evolution and mechanical properties of diffusion bonding high Nb containing TiAl alloy to Ti_2AlNb alloy [J]. Vacuum, 2019, 164: 140−148.
[29] WANG Y, CAI X Q, YANG Z W, WANG D P, LIU X G, LIU Y C. Diffusion bonding of Ti_2AlNb alloy using pure Ti foil as an interlayer [J]. Journal of Alloys and Compounds, 2018, 756: 163−174.
[30] REN H S, REN X Y, XIONG H P, LI W W, PANG S J, USTINOV A I. Nano-diffusion bonding of Ti_2AlNb to Ni-based superalloy [J]. Materials Characterization, 2019, 155: 109813.
[31] WANG Zi-chen, LI Chun, QI Jun-lei, FENG Ji-cai, CAO Jian. Characterization of hydrogenated niobium interlayer and its application in TiAl/Ti_2AlNb diffusion bonding [J]. International Journal of Hydrogen Energy, 2019, 44: 6929−6937.
[32] ZHAO Y Q, XIN S W, ZENG W D. Effect of major alloying elements on microstructure and mechanical properties of a highly β stabilized titanium alloy [J]. Journal of Alloys and Compounds, 2009, 481: 190−194.
[33] HUANG S, ZHANG J, MA Y, ZHANG S, YOUSSEF S S, QI M, WANG H, QIU J, XU D, LEI J, YANG R. Influence of thermal treatment on element partitioning in α+β titanium alloy [J]. Journal of Alloys and Compounds, 2019, 791: 575−585.
[34] SHA Jian-jun, LÜ Zhao-zhao, SHA Ru-yi, ZU Yu-fei, DAI Ji-xiang, XIAN Yu-qiang, ZHANG Wei, CUI Ding, YAN Cong-lin. Improved wettability and mechanical properties of metal coated carbon fiber-reinforced aluminum matrix composites by squeeze melt infiltration technique [J]. Transactions of Nonferrous Metals Society of China, 2021, 31(2): 317−330.
[35] FENG G, LI Z, ZHOU Z, YANG Y, ZACHARIAH M R. Microstructure and mechanical properties of C_f/Al−TiAl laser-assisted brazed joint [J]. Journal of Materials Processing Technology, 2017, 255: 195−203.
[36] FENG Guang-jie, LI Zhuo-ran, XU Xiao-long, SHEN Zhong-ke, YANG Yong. Glass−copper anodic bonding through activated Sn−0.6Al solder [J]. Journal of Materials Processing Technology, 2018, 254: 108−113.
[37] YAO Qing, CHENG Hui-chao, FAN Jing-lian, YAN Hai-xiang, ZHANG Cheng-gong. High strength Mo/Ti6Al4V diffusion bonding joints: Interfacial microstructure and mechanical properties [J]. International Journal of Refractory Metals and Hard Materials, 2019, 82: 159−166.
[38] FENG Guang-jie, LI Zhuo-ran, ZHOU Zhi, WANG Yu. Joining of C_f/Al composites and TiAl intermetallics by laser-induced self-propagating high-temperature synthesis using the Ni−Al−Zr interlayer [J]. Materials & Design, 2016, 110: 130−137.
[39] LI Zhuo-ran, FENG Guang-jie, WANG Shi-yu, FENG Shi-cheng. High-efficiency joining of C_f/Al composites and TiAl alloys under the heat effect of laser-ignited self-propagating high-temperature synthesis [J]. Journal of Materials Science & Technology, 2016, 32: 1111−1116.
[40] FENG Guang-jie, LI Zhuo-ran, FENG Shi-cheng, SHEN Zhong-ke. Effect of Ti–Al content on microstructure and mechanical properties of C_f/Al and TiAl joint by laser ignited self-propagating high-temperature synthesis [J]. Transactions of Nonferrous Metals Society of China, 2015, 25(5): 1468−1477.

Ti_2AlNb 合金与 TC4 合金真空扩散连接

冯广杰[1]，魏 岩[1]，胡丙旭[1]，王义峰[1]，邓德安[1]，杨秀霞[2]

1. 重庆大学 材料科学与工程学院，重庆 400044；
2. 江西农业大学 国土资源与环境学院，南昌 330045

摘 要：采用真空扩散焊方法连接 Ti_2AlNb 合金与 TC4 合金，并研究连接参数与接头显微组织、力学性能之间的关系。结果表明，由于 Al、Ti、Nb 和 V 的扩散，界面处生成 3 种反应层，分别是 TC4 一侧的 $B2/\beta$ 层和 α_2 层以及 Ti_2AlNb 侧的 α_2+$B2/\beta$ 层。连接温度决定接头中的原子活性，因此，控制着反应层的形成和接头的抗剪切强度。当连接温度为 950 ℃、保温时间为 30 min 和连接压力为 10 MPa 时，接头的抗剪切强度达到最高，为 467 MPa。断口形貌的分析结果表明，断裂主要发生在 $B2/\beta$ 层，接头的断裂模式为韧性断裂。同时，对接头的形成机理进行系统深入的讨论。

关键词：Ti_2AlNb 合金；TC4 合金；扩散连接；界面反应；抗剪切强度；形成机理

(Edited by Bing YANG)